Hindawi Publishing Corporation
Journal of Nanomaterials
Volume 2015, Article ID 703632, 8 pages
http://dx.doi.org/10.1155/2015/703632

Research Article

Comparison of Oxidative Stresses Mediated by Different Crystalline Forms and Surface Modification of Titanium Dioxide Nanoparticles

Karim Samy El-Said,[1,2] Ehab Mostafa Ali,[2] Koki Kanehira,[3] and Akiyoshi Taniguchi[1,4]

[1]*Cell-Material Interaction Group, Biomaterial Unit, Nano-Bio Field, Interaction Center for Material Nanoarchitectonics (MANA), National Institute for Materials Science (NIMS), Ibaraki 305-0044, Japan*
[2]*Department of Chemistry, Faculty of Science, Tanta University, Tanta, Egypt*
[3]*Biotechnology Group, TOTO Ltd. Research Institute, Honson 2-8-1, Chigasaki, Kanagawa 253-8577, Japan*
[4]*Graduate School of Advanced Science and Engineering, Waseda University, Tokyo 169-8555, Japan*

Correspondence should be addressed to Akiyoshi Taniguchi; taniguchi.akiyoshi@nims.go.jp

Received 5 February 2015; Accepted 30 March 2015

Academic Editor: Dongwoo Khang

Titanium dioxide nanoparticles (TiO_2 NPs) are manufactured worldwide for use in a wide range of applications. There are two common crystalline forms of TiO_2 anatase and rutile with different physical and chemical characteristics. We previously demonstrated that an increased DNA damage response is mediated by anatase crystalline form compared to rutile. In the present study, we conjugated TiO_2 NPs with polyethylene glycol (PEG) in order to reduce the genotoxicity and we evaluated some oxidative stress parameters to obtain information on the cellular mechanisms of DNA damage that operate in response to TiO_2 NPs different crystalline forms exposure in hepatocarcinoma cell lines (HepG2). Our results indicated a significant increase in oxidative stress mediated by the anatase form of TiO_2 NPs compared to rutile form. On the other hand, PEG modified TiO_2 NPs showed a significant decrease in oxidative stress as compared to TiO_2 NPs. These data suggested that the genotoxic potential of TiO_2 NPs varies with crystalline form and surface modification.

1. Introduction

With the development of nanotechnology, there has been a tremendous growth in the application of nanoparticles (NPs) for drug delivery systems, antibacterial materials, cosmetics, sunscreens, and electronics [1, 2]. The increased generation, use, and disposal of nanomaterial-containing products have led to an increase in the potential exposure risk to nanomaterials for both humans and the environment [3]. Titanium dioxide (TiO_2) NPs rank among the top five NPs used in consumer products [4]. TiO_2 NPs are produced abundantly and used widely because of their high stability and anticorrosive and photocatalytic properties [5]. TiO_2 is believed to be chemically inert. However, when the particles become progressively smaller, their surface areas, in turn, become progressively larger. Researchers have also expressed concerns about the harmful effects of TiO_2 NPs on human health, which are associated with this decrease in particle size [6, 7].

TiO_2 naturally occurs in several crystalline forms, of which the most commonly found forms are anatase and rutile. The principal parameters of particles affecting their physicochemical properties include shape, size, surface characteristics, and inner structure. It has been suggested that anatase TiO_2 has a greater toxic potential than rutile TiO_2 [8, 9]. The rutile form of TiO_2 NPs is highly effective in the absorption of ultraviolet radiation and thus is used in sunscreens to protect against UV-induced skin damage. In contrast, the anatase form is widely used as a photocatalyst at visible or ultraviolet wavelengths [10]. The anatase form can also oxidize oxygen or organic materials directly, with active TiO_2 NP photocatalysis in aqueous media generating reactive

oxygen species (ROS) such as superoxide (O_2^-), hydroxyl radical ($HO^\bullet$), hydrogen peroxide (H_2O_2), and singlet oxygen [11, 12]. The excess ROS can damage cellular lipids, proteins, or DNA, thus inhibiting their normal function. Because of this, oxidative stress has been implicated in a number of human diseases, as well as in the ageing process. While ROS are products of normal cellular metabolism, they are also known to play a deleterious role in living systems [13].

Surface modification, such as coating, influences the activity of TiO_2 NPs. For example, diminished cytotoxicity was observed when the surface of TiO_2 NPs was modified by a "grafting-to" polymer technique combining catalytic chain transfer and thiol-ene click chemistry [14]. Polyethylene glycol (PEG) is nontoxic and nonimmunogenic and has favorable pharmacokinetics and tissue distribution [15]. PEG is a hydrophilic, nonionic polymer that exhibits excellent biocompatibility [16]. When used for drug delivery purposes, the addition of PEG to polymer particles results in increased circulation time, which in turn prevented NPs uptake by the reticuloendothelial system [17]. PEG increases hydrophilic properties and porosity and decreases crystal size and the potential for cracked film formation [18]. A water-dispersed, PEG-modified TiO_2 nanoparticles exhibited photocatalytic antitumor effects in a glioma cell line [19].

In previous study, we demonstrated that an increased DNA damage response is mediated by the anatase crystalline form compared to rutile and mixed forms [20] and that PEG-TiO_2 NPs showed a reduction in DNA damage responses compared to TiO_2 NPs [21]. We also showed that TiO_2 NPs induced ROS, which are implicated in the genotoxicity induced by TiO_2 NPs [22]. However, the molecular mechanism of the DNA damage induced by the different crystalline forms of TiO_2 NPs is unknown. In this study, we explored whether the different crystalline forms of TiO_2 NPs cause distinct oxidative stress responses due to differences in their photocatalytic characteristics by measuring oxidative and antioxidative parameters and studied also the effect of PEG conjugation of TiO_2 NPs on oxidative stress in HepG2 cells. The results indicate that the anatase form exposure induced ROS generation with increased H_2O_2, decreased glutathione peroxidase, and reduced glutathione levels more than rutile forms; this effect is followed by release of cytochrome c from mitochondria to cytoplasm, increased caspase-3 activity, and caused eventual DNA fragmentation and apoptosis in cells treated with TiO_2 NPs anatase form more than rutile forms. PEG-modified TiO_2 NPs treated HepG2 cells showed a reduction in oxidative stress and apoptosis compared with cells exposed to different forms of TiO_2 NPs. We anticipate that our work will advance the understanding of interactions between bionanomaterials and mammalian cells, thereby improving their application in biology and medicine.

2. Materials and Methods

2.1. Cells and Cell Culture. HepG2 cells were cultured in Dulbecco's Modified Eagle's Medium (DMEM, Nacalai Tesque, Inc., Kyoto, Japan) supplemented with 10% fetal bovine serum (FBS, Biowest, Nuaillé, France, UK), 100 U/mL penicillin, and 100 μg/mL streptomycin (Nacalai Tesque, Inc.) at 37°C in a humidified atmosphere containing 5% CO_2.

2.2. Preparation and Exposure to TiO_2 and PEG-TiO_2 NPs. The preparation and characterization of TiO_2 NPs were described in previous studies [23, 24]. Briefly, raw titanium (IV) oxide nanoparticles of different forms (rutile, anatase, mixed rutile, and anatase) were purchased from Sigma-Aldrich (St. Louis, MO, USA). Mixed TiO_2 samples contained approximately 80% anatase and 20% rutile form. TiO_2 NPs were dispersed in distilled water and autoclaved at 120°C for 20 min. After cooling to room temperature, the TiO_2 NP suspensions were sonicated for 10 min at 200 kHz using a high frequency ultrasonic sonicator (MidSonic 600; Kaijo, Japan). The concentration of TiO_2 NPs in the samples was determined using a UV-VIS spectrophotometer at 340 nm (UV-1600; Shimadzu, Kyoto, Japan). All samples were stored at 4°C until use. TiO_2 NPs were adjusted to the desired concentration just before use by adding cell culture medium supplemented with 10% FBS (as above). In order to characterize TiO_2 NPs under cell culture conditions, the TiO_2 NPs were dispersed into the culture medium and subjected to the same cell culture conditions as above. Then, particle size distribution and zeta potential of the TiO_2 NP solutions were measured by dynamic light scattering (Zetasizer Nano-ZS; Malvern Instruments, Malvern, UK). Prior to addition to the cell cultures, the suspensions of TiO_2 NPs were diluted in supplemented medium and used at a final concentration of 10 μg/mL as described above. PEG-modified TiO_2 NPs (PEG-TiO_2) were prepared as described previously [19]. Specifically, TiO_2 or PEG-TiO_2 NPs were added to the culture medium immediately before the medium was applied to the cells. After a 48 h incubation period, the cells were harvested and assayed.

2.3. DCF Assay for Oxidative Stress Determination. The accumulation of intracellular free radicals from HepG2 cells exposed to different forms of TiO_2 and PEG-modified TiO_2 NPs was quantified using a ROS Assay Kit (OxiSelect; Cell Biolabs, Inc., San Diego, CA, USA), with the cell-permeable fluorogenic probe 2′,7′-dichlorodihydrofluorescein diacetate (DCFH-DA). DCFH-DA is a ROS detector that can cross cell membranes and be deacetylated by intracellular esterases to nonfluorescent 2′,7′-dichlorodihydrofluorescein (DCFH). In the presence of ROS, DCFH is rapidly oxidized to the highly fluorescent DCF, which is readily detectable. The fluorescence intensity is proportional to the ROS levels within the cell cytosol. HepG2 cells were cultured in 96-well black plates overnight. The cells were treated with different forms of TiO_2 NPs (anatase, rutile, mixed) and PEG-TiO_2 NPs for 48 h and were then incubated with DCHF-DA for 30 min at 37°C in the dark. Parallel sets of wells containing freshly cultured cells not treated with nanoparticles and suspended in the same concentration ratio of DPBS and DMEM were used as the negative controls. The fluorescence emission of DCF was monitored at regular intervals at an excitation wavelength of 480 nm and an emission wavelength of 530 nm using a fluorescence plate reader (Twinkle LB 970 Microplate Fluorometer; Berthold Technologies GmbH & Co. KG, Bad Wildbad, Germany). The amount of DCF formed was calculated from a calibration curve constructed using an authentic DCF standard.

2.4. Measurement of Glutathione Peroxidase (GPX). Glutathione peroxidase activity was measured using a Glutathione Peroxidase Assay Kit (Cayman Chemical Company, Ann Arbor, MI, USA). Cells were washed in phosphate buffer (pH 7.4) and collected by centrifugation (2000 ×g for 10 min at 4°C). Cells were homogenized in cold assay buffer (50 mM Tris-HCl, pH 7.5, 5 mM EDTA, and 1 mM DTT), centrifuged at 10,000 ×g for 15 min at 4°C, and the supernatant was used for the assay. Assay buffer (100 μL), 50 μL of cosubstrate mixture, and 20 μL of sample were placed in the wells of a 96-well plate, and the reaction was initiated by adding 20 μL of cumene hydroperoxide. The samples were thoroughly mixed by shaking and the absorbance was read at a minimum of 5 time points at 340 nm using a plate reader.

2.5. Measurement of Reduced Glutathione (GSH). The total glutathione concentration (reduced and oxidized forms) was determined in a microtitre plate assay using a Glutathione Assay Kit (Sigma-Aldrich). After nanoparticle exposure, HepG2 cells were washed twice with phosphate-buffered saline (PBS), resuspended in 5% 5-sulfosalicylic acid solution, and then centrifuged at 10,000 ×g for 10 min. A 10 μL aliquot of supernatant was mixed with 150 μL of working solution and incubated for 5 minutes at room temperature, and then 50 μL of diluted NADPH solution was added. The absorbance was measured at 412 nm using a plate reader, subtracting each reading from the reagent blank (10 μL of 5% 5-sulfosalicylic acid instead of sample). The final concentration of the components in the reaction mixture was 95 mM potassium phosphate buffer (pH 7.0) containing 0.95 mM ethylenediamine tetra-acetic acid (EDTA), 0.038 mg/mL (48 μM) NADPH, 0.031 mg/mL DTNB, 0.115 units/mL glutathione reductase, and 0.24% 5-sulfosalicylic acid. All measurements were performed in triplicate; GSH content (nmoles) could be calculated in the unknown samples.

2.6. Measurement of Caspase-3. A Caspase-3 Assay Kit (Colorimetric; Sigma-Aldrich) was used to assess caspase-3 activity. HepG2 cells (1×10^6) were cultured in 6-well plates and treated as described above. At the end of the experiment, cells were washed and lysed in 100 μL of lysis buffer. Next, 80 μL of the sample was added to 10 μL of 10x assay buffer and 10 μL of 2 mM Ac-DEVD-pNA chromogenic substrate in the wells of a 96-well plate. Samples were incubated for 10 hours at 37°C, and absorbance was read at 405 nm.

2.7. Confocal Microscopy Observation. Confocal laser scanning microscopy was performed using a Zeiss LSM510 microscope (Carl Zeiss, Oberkochen, Germany). On the following day, the culture medium was replaced with medium containing the two crystalline forms of TiO_2 NPs (anatase or rutile) at 10 μg/mL. Cells without NP exposure were used as controls. After a 48-h incubation, the cells were washed with PBS and fixed with 4% paraformaldehyde for 5 min. Fixed cells were then stained for nuclei with 1 μg/mL Hoechst 33342 (Dojin Chemical, Tokyo Japan) for 30 min at 5% CO_2. Figures were created using NIH ImageJ software.

2.8. Statistical Analysis. Data were expressed as the mean ± S.D. ($n \geq 3$ independent experiments). The data were analyzed using one-way analysis of variance (ANOVA) to evaluate the statistical differences and multicomparison between treated and control cells. Statistical significance was accepted at $P < 0.05$.

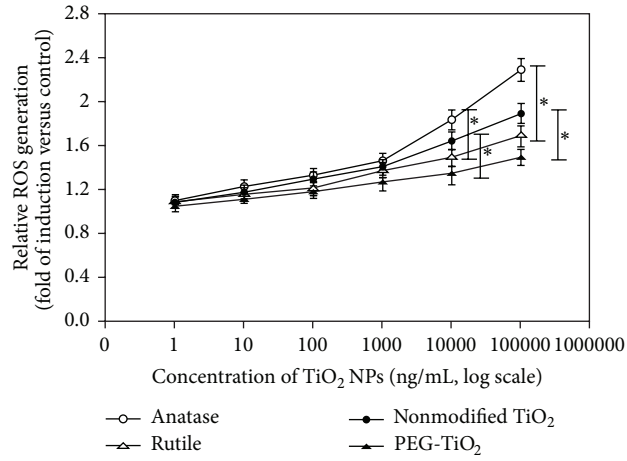

Figure 1: ROS generation by different crystalline forms of TiO_2 NPs in HepG2 cells. HepG2 cells were exposed to the anatase and rutile forms of TiO_2 NPs, as well as nonmodified mixed crystalline TiO_2 NPs (nonmodified TiO_2) and the crystalline form of PEG modified TiO_2 NPs (PEG-TiO_2). Cells were exposed to the TiO_2 NPs for 48 h at the indicated concentrations. The results are normalized to values obtained from control HepG2 cells without NP exposure. Each plot was produced from triplicate measurements, with values presented as mean ± S.D. ($^*P < 0.05$).

3. Results and Discussion

3.1. ROS Generation by Different Forms of TiO_2 NPs. In the present study, we compared the oxidative stress induced by the different crystalline forms of TiO_2 NPs (anatase and rutile) and different surface forms, that is, nonmodified mixed crystalline form (nonmodified TiO_2) and PEG-modified mixed crystalline form (PEG-TiO_2) of TiO_2 NPs. HepG2 cells were exposed to the various TiO_2 NPs and ROS generation was evaluated according to dose dependency (Figure 1) and time (Figure 2). We used different concentrations of NPs ranging from 1 ng/mL to 100 μg/mL and exposure times ranging from 3 h to 48 h. Cells not exposed to NPs were used as controls. Our results showed that TiO_2 NPs-induced ROS were generated in a dose-dependent manner. At low NPs concentrations (1 to 1000 ng/mL), significant levels of ROS were not generated in response to NPs exposure. However, cells treated with 10 and 100 μg/mL of anatase TiO_2 NPs showed a significant increase in ROS generation as compared to cells treated with rutile form of TiO_2 NPs. Changing the surface characters of TiO_2 NPs by coating with PEG (PEG-TiO_2) showed significantly less ROS generation when compared with the nonmodified mixed form of TiO_2 NPs (nonmodified TiO_2) as shown in Figure 1.

Figure 2 shows the time course of ROS generation following treatment with the different types of TiO_2 NPs; the concentration of NPs was standardized at 10 μg/mL. At 48 h of NPs exposure, each NP caused a significant increase in

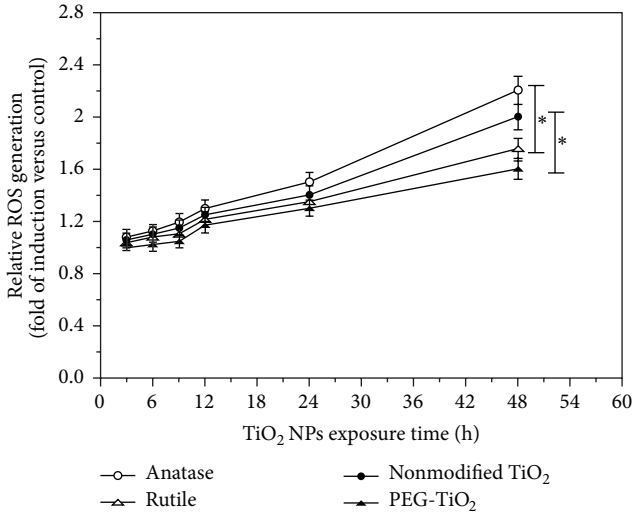

Figure 2: Time course of ROS generation in HepG2 cells exposed to different types of TiO_2 NPs. The cells were exposed to NPs (10 μg/mL) for the indicated durations. The results are normalized to values obtained from control HepG2 cells without NP exposure. Each plot was produced from triplicate measurements, with values presented as mean ± S.D. ($^*P < 0.05$).

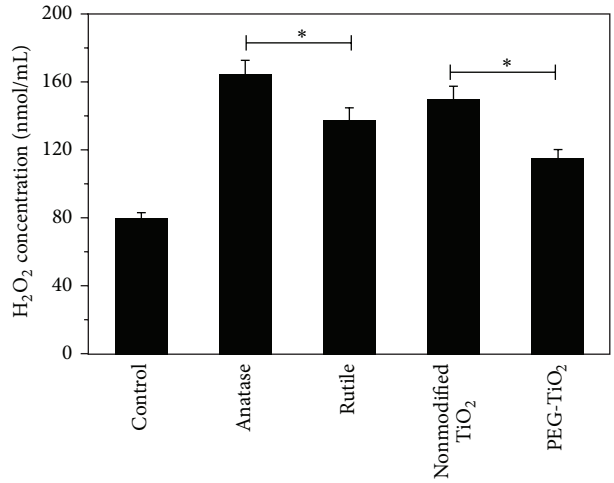

Figure 3: Measurement of H_2O_2 concentrations in HepG2 cells exposed to different types of TiO_2 NPs. Cells were exposed to individual NPs (10 μg/mL) for 48 h. HepG2 cells without NP exposure are shown as control. Each plot was produced from triplicate measurements, with values presented as mean ± S.D. ($^*P < 0.05$).

ROS generation; cells exposed to anatase TiO_2 NPs forms showed a 2.2-fold increase, while cells exposed to rutile TiO_2 NPs showed an approximately 1.75-fold increase. The nonmodified TiO_2 NPs mixed forms exposed cells exhibited 2-fold increase and the PEG-TiO_2 NPs treated cells showed 1.6-fold increase in ROS generation compared to the control cells. There was no effective change on the ROS generation of HepG2 cells when exposed to shorter times to NPs. These results indicate that cells treated with anatase form exhibited significantly more ROS generation when compared with cells treated with the rutile form and that PEG modification causes a significant decrease in ROS generated by mixed TiO_2 NPs. Therefore, the crystalline form and surface characters of TiO_2 NPs are an important point to investigate when studying the interaction of the nanomaterials with cells.

3.2. Oxidative Stress Determinations. Oxidative stress is described as the deregulation of oxidants and antioxidants, which is associated with several diseases. Hydrogen peroxide (H_2O_2) is a main ROS that is produced endogenously by several physiological processes, such as the inflammatory respiratory burst and during oxidative phosphorylation. ROS, including H_2O_2, also participate in pathway signaling related to cellular proliferation, migration, and apoptosis [25]. Figure 3 shows H_2O_2 induction by different types of TiO_2 NPs exposure. HepG2 cells exposed to the anatase form showed an approximately 2-fold significant increase in H_2O_2 levels (reaching 165 nmol/mL) compared to control cells. The cells exposed to rutile TiO_2 NP generated 138 nmol/mL of H_2O_2, an approximately 1.7-fold significant increase when compared to control cells, and the H_2O_2 level in cells exposed to nonmodified TiO_2 NPs mixed form was 150 nmol/mL, an approximately 1.8-fold significant increase compared to control cells. PEG-TiO_2 NPs exposed cells showed a significant decrease in H_2O_2 levels (115 nmol/mL) compared with nonmodified mixed forms of TiO_2 NPs; the one-way analysis of variance (ANOVA) and multicomparison between all treated cells and control cells showed that the variation of means is significantly increased and P value is less than 0.05. The data suggested that HepG2 cells exposed to TiO_2 NP showed H_2O_2-induced oxidative stress, and exposure to anatase TiO_2 NPs caused significantly higher responses to H_2O_2-induced oxidative stress than rutile TiO_2 NPs forms exposure and PEG modification of TiO_2 NPs protected HepG2 cells against H_2O_2-induced oxidative stress.

Antioxidant activities in HepG2 cells exposed to different types of TiO_2 NPs were evaluated by measuring GPX activity and GSH levels. GPX is the enzyme that catalyzes the reduction of hydroperoxides, including H_2O_2. GPX activity and GSH levels were evaluated to elucidate the mechanism of H_2O_2 detoxification during exposure to different types of TiO_2 NPs. The results indicate that cells exposed to anatase, rutile, and nonmodified TiO_2 NPs exhibited 38, 50, and 40 nmol/min/mL of GPX activity, respectively. HepG2 cells treated with anatase TiO_2 NPs showed significantly less GPX activity, indicating increased oxidative stress compared to cells exposed to the rutile forms. Cells exposed to PEG-TiO_2 exhibited a significantly more GPX activity (58 nmol/min/mL), indicating retention of antioxidant capacity (Figure 4). The multicomparison data between all treated cells and control showed significant changes except cells exposed to anatase versus cells exposed to nonmodified TiO_2 NPs which showed nonsignificant change with P value greater than 0.05.

Similarly, HepG2 cells exposed to TiO_2 NP exhibited reduced GSH levels. Specifically, cells exposed to anatase TiO_2 NPs exhibited significantly decreased GSH levels compared to cells treated with rutile forms. PEG-TiO_2 NPs

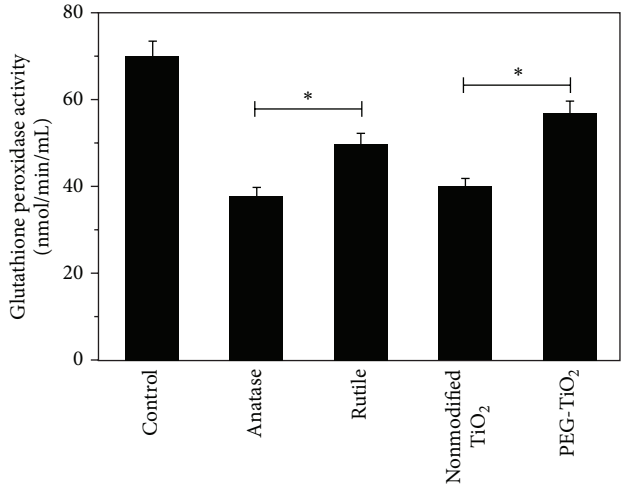

Figure 4: GPx activities in HepG2 cells exposed to different types of TiO_2 NPs. Cells were exposed to individual NPs (10 μg/mL) for 48 h. Control values represent HepG2 cells without NP exposure. Each plot was produced from triplicate measurements, with values presented as mean ± S.D. ($^*P < 0.05$).

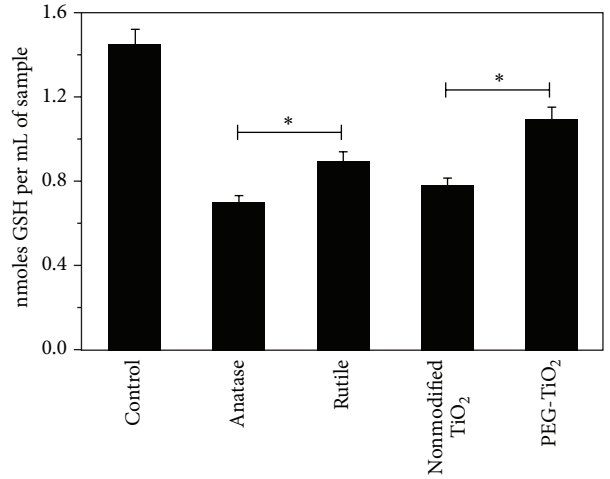

Figure 5: GSH levels in HepG2 cells exposed to different types of TiO_2 NPs. Cells were exposed to individual NPs (10 μg/mL) for 48 h. Control values represent HepG2 cells without NP exposure. Each plot was produced from triplicate measurements, with values presented as mean ± S.D. ($^*P < 0.05$).

appeared to reduce the effects of TiO_2 NP exposure and increased GSH levels (Figure 5). Statistical analysis of GSH data and comparison between cells showed that significant changes between cells only were observed in control versus anatase exposed cells $^{***}P < 0.001$, control versus rutile $^{**}P < 0.01$, control versus nonmodified $^{**}P < 0.01$, and anatase versus PEG-modified treated cells $^*P < 0.05$. These results suggest that the antioxidant GSH is involved in H_2O_2 detoxification following TiO_2 NPs exposure and that anatase TiO_2 produces greater oxidative stress than rutile TiO_2, as evidenced by their effects on GSH levels.

3.3. Assessments of Oxidative Stress-Induced Apoptosis. Caspase-3 is an effector cysteine protease that is involved in apoptosis and necrosis and is activated by H_2O_2 [26]. Caspase-3 activity was measured to evaluate the apoptotic responses to oxidative stress occurring in HepG2 cells exposed to different forms of TiO_2 NPs. Our results showed a significant increase in caspase-3 activity, which is a critical apoptotic enzyme, as well as DNA fragmentation, in cells exposed to anatase TiO_2 NPs (3.2 and 2.5 nmol/min/mL in anatase and rutile NPs, resp.). Nonmodified TiO_2 NP exposure produced 2.7 nmol/min/mL of caspase-3 activity, while PEG-TiO_2 NP-treatment resulted in 2.1 nmol/min/mL, which is virtually the same as the control value of 2 nmol/min/mL (Figure 6). The significant changes between cells were observed in control versus anatase $^{**}P < 0.01$, anatase versus rutile $^*P < 0.05$, and anatase versus PEG-modified treated cells $^{***}P < 0.001$. Therefore, anatase TiO_2 NPs produced significantly greater apoptotic responses than the rutile form in HepG2 cells.

The induction of apoptosis in HepG2 cells exposed to the two common crystalline forms of TiO_2 NPs was confirmed by observing apoptotic cells using confocal microscopy. We used Hoechst DNA staining to observe nuclear fragmentation as an indication of apoptosis. The morphological

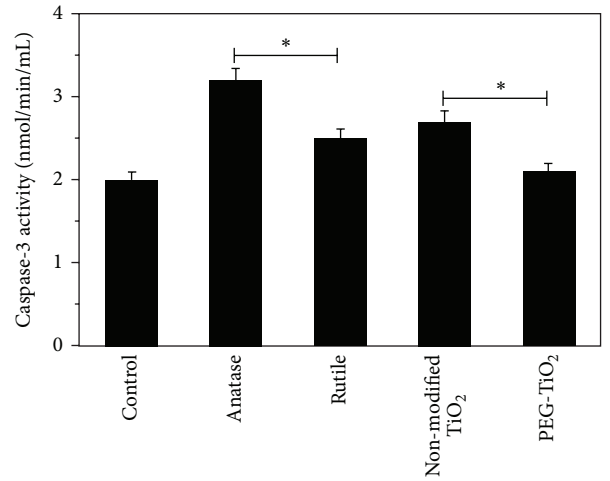

Figure 6: Caspase-3 activity in HepG2 cells exposed to different types of TiO_2 NPs. Cells were exposed to individual NPs (10 μg/mL) for 48 h. Control values represent HepG2 cells without NP exposure. Each plot was produced from triplicate measurements, with values presented as mean ± S.D. ($^*P < 0.05$).

changes observed include condensation of chromatin and nuclear fragmentation, as shown in Figure 7. The microscopy analysis confirmed that cells exposed to TiO_2 NPs undergo programmed cell death (apoptosis) due to DNA damage. Enumeration of apoptotic HepG2 cells in the absence of TiO_2 NPs revealed the percentage of cells with nuclear fragmentation to be 30% (Figure 7(a)), while 71% of HepG2 cells exposed to crystalline anatase TiO_2 NPs (Figure 7(b)) and 59% of cells exposed to rutile TiO_2 NPs were apoptotic (Figure 7(c)). The results indicate that the crystalline anatase TiO_2 NPs induce a greater degree of apoptotic cell death compared with the rutile form.

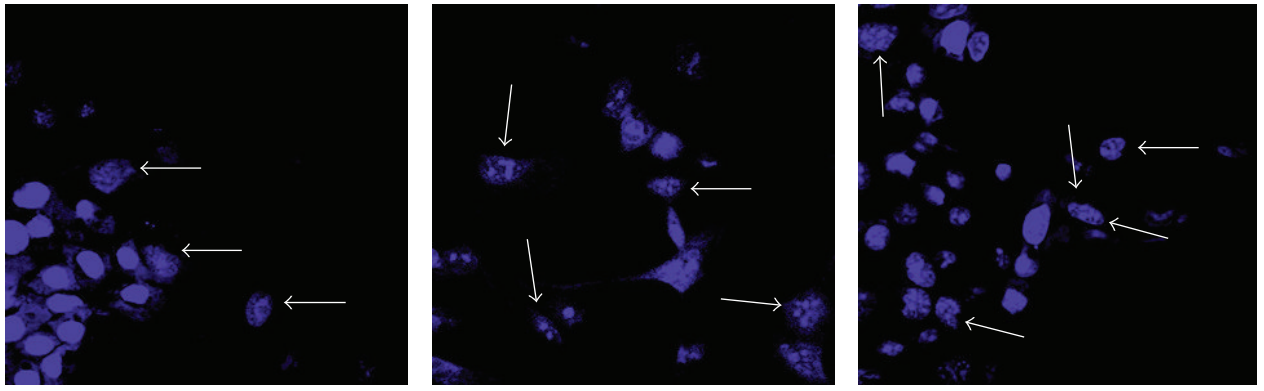

(a) (b) (c)

Figure 7: Confocal laser scanning microscopic images of HepG2 cells exposed to TiO_2 NPs. The confocal microscopic images show condensation of chromatin and nuclear fragmentation in HepG2 cells exposed to different crystalline forms of TiO_2 NPs. (a) Control HepG2 cells without TiO_2 NPs exposure; (b) cells exposed to 10 μg/mL crystalline anatase TiO_2 NPs for 48 h; (c) cells exposed to 10 μg/mL crystalline rutile TiO_2 NPs for 48 h. The white arrows indicate apoptotic cells with nuclear fragmentation.

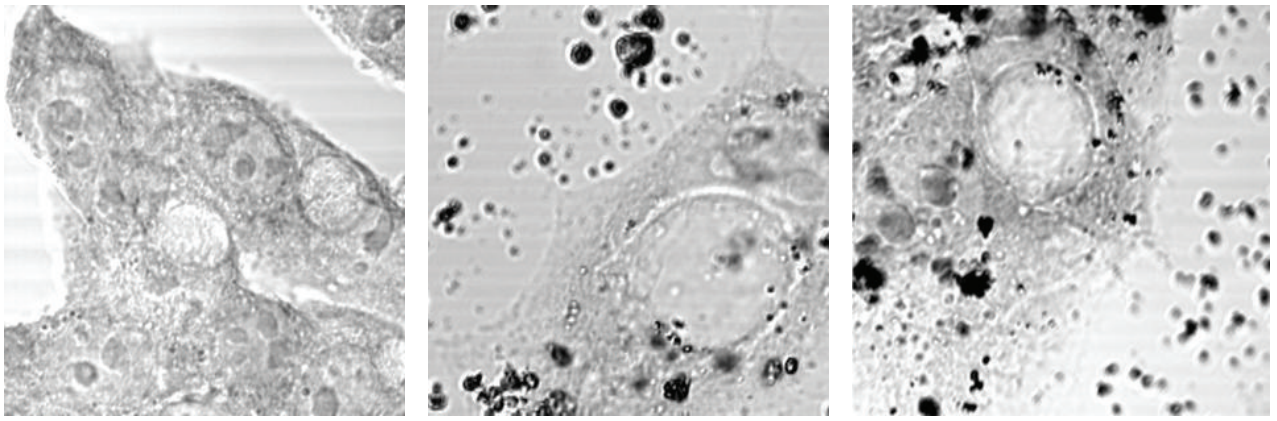

(a) (b) (c)

Figure 8: Localization of crystalline anatase and rutile TiO_2 NPs in HepG2 cells. Confocal microscopy of reflection images was used also to verify the location of TiO_2 NPs in HepG2 cells. (a) Control HepG2 cells without TiO_2 NP exposure; (b) cells exposed to 10 μg/mL crystalline anatase TiO_2 NPs for 48 h; (c) cells exposed to 10 μg/mL crystalline rutile TiO_2 NPs for 48 h.

Confocal microscopy was used also to verify the location of TiO_2 NPs in HepG2 cells. The images revealed that anatase and rutile TiO_2 NPs were internalized by HepG2 cells to a similar degree (Figures 8(b) and 8(c)), when compared to control cells (Figure 8(a)). These results indicate that both crystalline forms of TiO_2 NPs were incorporated by HepG2 cells to the same extent.

4. Discussion

Generally, anatase is more reactive than rutile. Anatase differs from rutile in cleavage and the overall visible external shape because of structural differences. Although both forms are tetragonal, the different crystalline forms give rise to different physical and chemical characteristics such as hardness, refractive index, and photocatalytic ability. In the present study, we compared the effects of the anatase and rutile crystalline forms of TiO_2 NPs on cellular oxidative stress and apoptosis in HepG2 cells. One of the most discussed mechanisms underlying the biological effects of ambient particles is their ability to cause oxidative stress. The interactions of NPs with cell membranes result in the generation of ROS, and the resulting oxidative stress may cause a degradation of membrane lipids, an imbalance of intracellular calcium homeostasis, and DNA breakage [27, 28], which is considered an underlying molecular mechanism implicated in the cytotoxic, inflammatory, and DNA damaging effects of nanoparticles. Our results showed that anatase TiO_2 has a greater ROS potential (mainly H_2O_2) than rutile TiO_2.

Our study showed greater inhibition of GPX activity and GSH levels in HepG2 cells exposed to anatase TiO_2 than the rutile form. GPX and GSH are antioxidants used in the detoxification of H_2O_2 and their inhibition confirms the retention of H_2O_2. H_2O_2 is a natural source of oxidative damage in

cells, causing a spectrum of DNA lesions, including single and double strand breaks [29]. DNA damage due to H_2O_2 results from the production of the hydroxyl radical ($^{\bullet}OH$) in the presence of transition metal ions, such as iron, via the Fenton reaction. H_2O_2 can cause oxidative stress because it uses water channels to rapidly cross cell membranes and reach the nucleus where it can damage DNA. Caspases are a family of proteases that regulate cell death and are important mediators of apoptosis. Caspase-3 is a critical effector caspase that plays a central role in initiating nuclear apoptosis, including chromatin condensation, DNA fragmentation, and blebbing [30]. Our results showed a significant increase in caspase-3 activity in HepG2 cells exposed to anatase TiO_2 NPs and to a lesser degree by exposure to the rutile form. We hypothesized that the two forms of TiO_2 NPs would elicit different cellular oxidative stress responses because, compared to rutile, anatase has a lighter average effective mass of photogenerated electrons and holes. The lighter effective mass suggests that anatase TiO_2 particles exhibit faster migration of electrons and holes from the interior to its surface and hence greater ROS generation, compared to rutile [31]. Our results support the contention that there is no difference in the cellular incorporation of anatase and rutile TiO_2 NPs. Therefore, the differences in genotoxicity induced by the two crystalline forms of TiO_2 NPs were due to differences in the generation of oxidative stress, which initiates DNA damage and apoptosis in HepG2 cells.

One strategy to prevent the genotoxicity of TiO_2 nanoformulations is through the use of a PEG coating. Modifying the surface of NPs with PEG prevents agglomeration [32], renders NPs resistant to protein adsorption, and enhances their biocompatibility [33]. We conjugated the TiO_2 NPs with PEG to examine whether TiO_2 NP-induced oxidative stress was altered. The present results showed that ROS generation was reduced following PEG modification, as evidenced by reduced levels of H_2O_2, preservation of GPX and GSH levels, and decreased caspase-3 activation, thus confirming the decreased DNA damage and oxidative stress-induced apoptosis in HepG2 cells exposed to PEG-TiO_2 NPs compared to cells exposed to TiO_2 NPs.

5. Conclusions

Our results showed that HepG2 cells treated with different types of TiO_2 NPs produced distinct oxidative stress responses by affecting the oxidative balance. Specifically, exposure to anatase TiO_2 NPs produced significantly greater ROS formation, oxidative stress responses, and apoptosis, when compared to rutile TiO_2 NPs. Furthermore, modification of TiO_2 NPs with PEG showed decreased oxidative stress and apoptosis in HepG2 cells, thereby confirming the reduction of ROS induced by TiO_2 NPs. Therefore, exposure of HepG2 cells to TiO_2 NP causes an elevation in ROS levels and downregulates ROS scavengers associated with protection from DNA damage and apoptosis. Furthermore, anatase forms mediated these events to a greater degree than rutile forms of TiO_2 NPs.

Conflict of Interests

The authors declare that they have no conflict of interests.

Acknowledgment

This work was supported by Interaction Center for Material Nanoarchitectonics (MANA), National Institute for Materials Science (NIMS), Japan.

References

[1] E. R. Kisin, A. R. Murray, M. J. Keane et al., "Single-walled carbon nanotubes: geno- and cytotoxic effects in lung fibroblast V79 cells," *Journal of Toxicology and Environmental Health Part A: Current Issues*, vol. 70, no. 24, pp. 2071–2079, 2007.

[2] T. A. Robertson, W. Y. Sanchez, and M. S. Roberts, "Are commercially available nanoparticles safe when applied to the skin?" *Journal of Biomedical Nanotechnology*, vol. 6, no. 5, pp. 452–468, 2010.

[3] M. S. Olson and P. L. Gurian, "Risk assessment strategies as nanomaterials transition into commercial applications," *Journal of Nanoparticle Research*, vol. 14, no. 4, article 786, 2012.

[4] R. K. Shukla, V. Sharma, A. K. Pandey, S. Singh, S. Sultana, and A. Dhawan, "ROS-mediated genotoxicity induced by titanium dioxide nanoparticles in human epidermal cells," *Toxicology in Vitro*, vol. 25, no. 1, pp. 231–241, 2011.

[5] J. Riu, A. Maroto, and F. X. Rius, "Nanosensors in environmental analysis," *Talanta*, vol. 69, no. 2, pp. 288–301, 2006.

[6] C. Wang and Y. Li, "Interaction and nanotoxic effect of TiO_2 nanoparticle on fibrinogen by multi-spectroscopic method," *Science of the Total Environment*, vol. 429, pp. 156–160, 2012.

[7] P. O. Andersson, C. Lejon, B. Ekstrand-Hammarström et al., "Polymorph- and size-dependent uptake and toxicity of TiO_2 nanoparticles in living lung epithelial cells," *Small*, vol. 7, no. 4, pp. 514–523, 2011.

[8] C. Xue, J. Wu, F. Lan et al., "Nano titanium dioxide induces the generation of ROS and potential damage in HaCaT cells under UVA irradiation," *Journal of Nanoscience and Nanotechnology*, vol. 10, no. 12, pp. 8500–8507, 2010.

[9] J. Petković, B. Žegura, M. Stevanović et al., "DNA damage and alterations in expression of DNA damage responsive genes induced by TiO_2 nanoparticles in human hepatoma HepG2 cells," *Nanotoxicology*, vol. 5, no. 3, pp. 341–353, 2011.

[10] M. E. Kurtoglu, T. Longenbach, and Y. Gogotsi, "Preventing sodium poisoning of photocatalytic TiO_2 films on glass by metal doping," *International Journal of Applied Glass Science*, vol. 2, no. 2, pp. 108–116, 2011.

[11] J. C. Ireland, P. Klostermann, E. W. Rice, and R. M. Clark, "Inactivation of *Escherichia coli* by titanium dioxide photocatalytic oxidation," *Applied and Environmental Microbiology*, vol. 59, no. 5, pp. 1668–1670, 1993.

[12] R. Konaka, E. Kasahara, W. C. Dunlap, Y. Yamamoto, K. C. Chien, and M. Inoue, "Ultraviolet irradiation of titanium dioxide in aqueous dispersion generates singlet oxygen," *Redox Report*, vol. 6, no. 5, pp. 319–325, 2001.

[13] M. Valko, C. J. Rhodes, J. Moncol, M. Izakovic, and M. Mazur, "Free radicals, metals and antioxidants in oxidative stress-induced cancer," *Chemico-Biological Interactions*, vol. 160, no. 1, pp. 1–40, 2006.

[14] R. Tedja, M. Lim, R. Amal, and C. Marquis, "Effects of serum adsorption on cellular uptake profile and consequent impact of titanium dioxide nanoparticles on human lung cell lines," *ACS Nano*, vol. 6, no. 5, pp. 4083–4093, 2012.

[15] W. Wang, W. Xiong, J. Wan, X. Sun, H. Xu, and X. Yang, "The decrease of PAMAM dendrimer-induced cytotoxicity by PEGylation via attenuation of oxidative stress," *Nanotechnology*, vol. 20, no. 10, Article ID 105103, 2009.

[16] J. V. Jokerst, T. Lobovkina, R. N. Zare, and S. S. Gambhir, "Nanoparticle PEGylation for imaging and therapy," *Nanomedicine*, vol. 6, no. 4, pp. 715–728, 2011.

[17] G. B. Jacobson, E. Gonzalez-Gonzalez, R. Spitler et al., "Biodegradable nanoparticles with sustained release of functional siRNA in skin," *Journal of Pharmaceutical Sciences*, vol. 99, no. 10, pp. 4261–4266, 2010.

[18] T. Miki, K. Nishizawa, K. Suzuki, and K. Kato, "Preparation of thick TiO_2 film with large surface area using aqueous sol with poly(ethylene glycol)," *Journal of Materials Science*, vol. 39, no. 2, pp. 699–701, 2004.

[19] S. Yamaguchi, H. Kobayashi, T. Narita et al., "Sonodynamic therapy using water-dispersed TiO_2-polyethylene glycol compound on glioma cells: comparison of cytotoxic mechanism with photodynamic therapy," *Ultrasonics Sonochemistry*, vol. 18, no. 5, pp. 1197–1204, 2011.

[20] P. Chen and A. Taniguchi, "Detection of DNA damage response caused by different forms of titanium dioxide nanoparticles using sensor cells," *Journal of Biosensors & Bioelectronics*, vol. 3, article 129, 2012.

[21] K. S. El-Said, E. M. Ali, K. Kanehira, and A. Taniguchi, "Effects of toll-like receptors 3 and 4 induced by titanium dioxide nanoparticles in DNA damage-detecting sensor cells," *Journal of Biosensors & Bioelectronics*, vol. 4, article 144, 2013.

[22] K. El-Said, E. Ali, K. Kanehira, and A. Taniguchi, "Molecular mechanism of DNA damage induced by titanium dioxide nanoparticles in toll-like receptor 3 or 4 expressing human hepatocarcinoma cell lines," *Journal of Nanobiotechnology*, vol. 12, article 48, 2014.

[23] P. Chen, S. Migita, K. Kanehira, S. Sonezaki, and A. Taniguchi, "Development of sensor cells using NF-κB pathway activation for detection of nanoparticle-induced inflammation," *Sensors*, vol. 11, no. 7, pp. 7219–7230, 2011.

[24] P. Chen, K. Kanehira, S. Sonezaki, and A. Taniguchi, "Detection of cellular response to titanium dioxide nanoparticle agglomerates by sensor cells using heat shock protein promoter," *Biotechnology and Bioengineering*, vol. 109, no. 12, pp. 3112–3118, 2012.

[25] M. R. Brown, F. J. Miller Jr., W.-G. Li et al., "Overexpression of human catalase inhibits proliferation and promotes apoptosis in vascular smooth muscle cells," *Circulation Research*, vol. 85, no. 6, pp. 524–533, 1999.

[26] S. M. Piperakis, K. Kontogianni, G. Karanastasi, Z. Iakovidou-Kritsi, and M. M. Piperakis, "The use of comet assay in measuring DNA damage and repair efficiency in child, adult, and old age populations," *Cell Biology and Toxicology*, vol. 25, no. 1, pp. 65–71, 2009.

[27] J. M. Petruska, K. O. Leslie, and B. T. Mossman, "Enhanced lipid peroxidation in lung lavage of rats after inhalation of asbestos," *Free Radical Biology and Medicine*, vol. 11, no. 4, pp. 425–432, 1991.

[28] R. K. Shukla, A. Kumar, A. K. Pandey, S. S. Singh, and A. Dhawan, "Titanium dioxide nanoparticles induce oxidative stress-mediated apoptosis in human keratinocyte cells," *Journal of Biomedical Nanotechnology*, vol. 7, no. 1, pp. 100–101, 2011.

[29] A. R. Collins, "Oxidative DNA damage, antioxidants, and cancer," *BioEssays*, vol. 21, no. 3, pp. 238–246, 1999.

[30] A. G. Porter and R. U. Jänicke, "Emerging roles of caspase-3 in apoptosis," *Cell Death and Differentiation*, vol. 6, no. 2, pp. 99–104, 1999.

[31] J. Zhang, P. Zhou, J. Liu, and J. Yu, "New understanding of the difference of photocatalytic activity among anatase, rutile and brookite TiO_2," *Physical Chemistry Chemical Physics*, vol. 16, pp. 20382–20386, 2014.

[32] S. Matsumura, S. Sato, M. Yudasaka et al., "Prevention of carbon nanohorn agglomeration using a conjugate composed of comb-shaped polyethylene glycol and a peptide aptamer," *Molecular Pharmaceutics*, vol. 6, no. 2, pp. 441–447, 2009.

[33] W. Eck, G. Craig, A. Sigdel et al., "PEGylated gold nanoparticles conjugated to monoclonal F19 antibodies as targeted labeling agents for human pancreatic carcinoma tissue," *ACS Nano*, vol. 2, no. 11, pp. 2263–2272, 2008.